Combination of baicalein and miR-106a-5p mimics significantly alleviates IL-1β-induced inflammatory injury in CHON-001 cells

QINGTIAN XIANG, JIJUN WANG, TONGWEI WANG and HONGGUANG ZUO

Department of Orthopedic Surgery, Xiang Shui County People's Hospital, Yancheng, Jiangsu 224600, P.R. China

Abstract. Osteoarthritis (OA) induces inflammation and degeneration of all joint components, and as such, is a considerable source of disability, pain and socioeconomic burden worldwide. Baicalein (BAI) and microRNA (miR)-106a-5p suppress the progression of OA; however, the effects of BAI and miR-106a-5p for the combined treatment of OA are not completely understood. An *in vitro* OA model was established by treating CHON-001 cells with 20 ng/ml interleukin (IL)-1β. Cell Counting Kit-8 and flow cytometry assays were conducted to evaluate cell viability and apoptosis, respectively. Western blotting was performed to determine the expression levels of Bax, active caspase-3, Bcl-2, collagen I, collagen III, aggrecan, matrix metallopeptidase (MMP)-13, MMP-9, active Notch1 and transcription factor hes family bHLH transcription factor 1 (Hes1). The levels of IL-6 and tumor necrosis factor-α in the cell culture medium were quantified via ELISA. The present study revealed that treatment with BAI or miR-106a-5p mimic alleviated IL-1β-induced apoptosis, and BAI + miR-106a-5p combination treatment exerted enhanced anti-inflammatory effects compared with monotherapy. Furthermore, IL-1β-induced accumulation of collagen, collagen III, MMP-13 and MMP-9 in CHON-001 cells was reversed to a greater degree following combination treatment compared with monotherapy. Likewise, IL-1β-induced aggrecan degradation was markedly reversed by combination treatment. IL-1β-induced upregulation of active Notch1 and Hes1 in CHON-001 cells was also significantly attenuated by combined BAI + miR-106a-5p treatment. In conclusion, the results of the present study revealed that the combination of BAI and miR-106a-5p mimic significantly decreased IL-1β-induced inflammatory injury in CHON-001 cells, which may serve as a novel therapeutic strategy for OA.

Correspondence to: Dr Hongguang Zuo, Department of Orthopedic Surgery, Xiang Shui County People's Hospital, 94 Middle Guanhe Road, Yancheng, Jiangsu 224600, P.R. China
E-mail: zhg0800@163.com

Introduction

Osteoarthritis (OA) is a major cause of musculoskeletal disability worldwide, which is associated with significant loss of work and a high socioeconomic burden (1). The prevalence of symptomatic OA is as high as 5-7% in the adult population worldwide (2). As one of the typical 'wear and tear' diseases, OA is primarily caused by articular cartilage damage or loss (3,4). Articular cartilage consists of chondrocytes, which are the sole cell type present in cartilage and the surrounding extracellular matrix (5). During OA progression, the original chondrocyte phenotype is altered to accompany a loss of type II collagen and aggrecan, and an increase in type I and III collagen (6,7). Matrix metalloproteinases (MMPs) and interleukin (IL)-1β have been considered as vital components of cartilage degradation (8). IL-1β induces cartilage degradation by triggering the expression of MMP9, MMP13 and other proteases (8-10). Tumor necrosis factor-α (TNF-α) activates chondrocytes to further enhance the production of proinflammatory cytokines (11,12). In addition, due to the low metabolic activity of chondrocytes, articular cartilage has no intrinsic repair capabilities (3,13). Therefore, despite various strategies of OA management (14), there are no effective therapeutic strategies for the disease.

Notch is a single-pass transmembrane cell surface receptor that serves a vital role in vascular development and cell-cell communication (15,16). Notch is as an important regulator of chondrocyte proliferation during cartilage development (17). Evidence has shown that the expression levels of Notch family members are increased in chondrocytes during OA progression (18). Yu *et al* (19) indicated that microRNA (miRNA/miR)-9 could facilitate cartilage regeneration of OA in rabbits by mediating Notch signaling.

Baicalein (BAI) is isolated from *Scutellaria baicalensis Georgi* (8,20) and possesses anti-inflammatory (21), antioxidative (22) and anticarcinogenic properties (23,24). The anti-OA abilities of BAI have also been investigated in previous *in vitro* and *in vivo* studies (8,20,25). One study demonstrated that BAI triggers the expression of antiapoptotic genes and decreases the expression of proapoptotic and proinflammatory gene products in rat chondrocytes (20). Another study illustrated that BAI significantly reduces the expression of MMPs, inhibiting IL-1β-induced cartilage degradation *in vitro* and *in vivo* (8).

As a family of endogenous small non-coding RNAs, miRNAs are post-transcriptional modulators that serve a

pivotal role in regulating key cellular processes, including biogenesis and genomic organization, by preferentially binding to the 3' untranslated regions of target mRNAs (26-29). The regulatory functions of miRNAs during the pathogenesis of OA have been reported (30-32). Numerous miRNAs, including miR-30a, miR-29, miR-105, miR-146a, miR-221-3p and miR-145, are involved in regulating the pathogenesis of OA (32). For example, Guan *et al* (33) reported that miR-164a expression was decreased in OA lesions of human articular cartilage, and miR-146a-deficient mice developed early onset OA characterized by cartilage degeneration and osteophytes. Moreover, Hu *et al* (34) indicated that miR-145 attenuates TNF-α-induced cartilage matrix degradation. Moreover, the overexpression or intra-articular injection of miR-106a-5p attenuated the progression of OA *in vitro* and *in vivo*, respectively (32).

Although BAI and miR-106a-5p have been separately reported to reduce articular cartilage injury, the combined effect of BAI and miR-106a-5p is not completely understood. Therefore, the present study aimed to investigate the effects of BAI + miR-106a-5p combination therapy on the progression of OA using an *in vitro* chondrocyte injury model.

Materials and methods

Cell culture. The CHON-001 human chondrocyte cell line was obtained from American Type Culture Collection. Cells were cultured in DMEM (Gibco; Thermo Fisher Scientific, Inc.) supplemented with 10% FBS (Gibco; Thermo Fisher Scientific, Inc.) and 100 U/ml penicillin/streptomycin (Gibco; Thermo Fisher Scientific, Inc.) in a humidified incubator at 37˚C with 5% CO_2. To establish an *in vitro* OA model, $5x10^4$ CHON-001 cells were stimulated with recombinant human IL-1β (0, 5, 10 or 20 ng/ml) for 24 h at 37˚C (cat. no. SRP6169; Sigma-Aldrich; Merck KGaA).

Transfection. miR-106a-5p mimics and negative control (NC) were obtained from Shanghai GenePharma Co., Ltd. CHON-001 cells were seeded into 6-well plates and cultured overnight to ~70% confluence. Subsequently, $5x10^4$ CHON-001 cells were transfected with 10 nM miR-106a-5p mimics or 10 nM NC using Lipofectamine® 2000 (Invitrogen; Thermo Fisher Scientific, Inc.) for 24 h according to the manufacturer's protocol.

For combination treatment, $5x10^4$ CHON-001 cells were transfected with miR-106a-5p mimics (2, 4, 6 or 10 nM) for 24 h at 37˚C, and subsequently treated with 20 µM BAI (cat. no. 465119; Sigma-Aldrich; Merck KGaA) for a further 24 h at 37˚C. Cells were then stimulated with 20 ng/ml IL-1β for another 24 h at 37˚C to induce the OA phenotype.

Cell viability assay. CHON-001 cells were seeded into 96-well plates ($5x10^3$ cells/well) and incubated at 37˚C overnight. Following transfection and treatment with BAI and IL-1β, cell viability was assessed using the Cell Counting Kit-8 (CCK-8) assay (Beyotime Institute of Biotechnology) according to the manufacturer's protocol. Briefly, 10 µl CCK-8 solution was added to each well and incubated at 37˚C for 2 h. The absorbance of each well was measured at a wavelength of 450 nm using a microplate reader (Bio-Rad Laboratories, Inc.).

Flow cytometry. CHON-001 cells were seeded ($5x10^4$ cells/well) and cultured to ~80% confluence. Cells were treated with different concentrations of IL-1β (0, 5, 10 or 20 ng/ml) for 24 h 37˚C. Subsequently, early apoptotic, late apoptotic and necrotic cells were assessed using the Annexin V-FITC Apoptosis Staining Detection kit (Abcam) according to the manufacturer's protocol. Briefly, cells were harvested and centrifuged at 626 x g for 5 min at 4˚C. After rinsing twice with PBS, cells were centrifuged at 626 x g for 5 min at 4˚C. Subsequently, cells ($1x10^5$) were collected from each group, resuspended in binding buffer, and subsequently stained with 5 µl Annexin V-FITC and 5 µl propidium iodide for 5 min in the dark at room temperature. Within 1 h, cell apoptosis was assessed via flow cytometry using a BD FACSAria flow cytometer (BD Biosciences) and CellQuest Pro software (version 5.1; BD Biosciences).

ELISA. Following transfection and treatment with BAI and IL-1β, culture supernatants were collected from 6-well plates and then centrifuged for 10 min at 626 x g at 4˚C. Subsequently, cellular IL-6 (cat. no. ES4078) and TNF-α (cat. no. ELK1190) concentrations were determined using ELISA kits (ELK Biotechnology Co., Ltd.) according to the manufacturer's protocol. IL-6 and TNF-α concentrations in cell supernatants (100 µl) were assessed for the following groups: i) Control; ii) 20 ng/ml IL-1β; iii) 20 ng/ml IL-1β + 20 µM BAI; iv) 20 ng/ml IL-1β + miR-106a-5p mimics; and v) 20 ng/ml IL-1β + miR-106a-5p mimics + 20 µM BAI.

Reverse transcription-quantitative PCR (RT-qPCR). To confirm successful transfection of miR-106a-5p mimics, total RNA was extracted from transfected CHON-001 cells using TRIzol® reagent (Invitrogen; Thermo Fisher Scientific, Inc.) Total RNA was reverse transcribed into cDNA using M-MLV Reverse Transcriptase (Invitrogen; Thermo Fisher Scientific, Inc.) according to the manufacturer's instructions. The RT reaction comprised the following: 1 µg RNA, 10 µl reaction solution, 1 µl RT primers and 1 µl dNTPs in a final volume of 15 µl. The mixture was heated at 70˚C for 5 min and then it was quickly placed on ice to cool. Subsequently, 4 µl RT buffer, 1 µl M-MLV Reverse Transcriptase and 1 µl RNase inhibitor were added into the mixture on ice. The RT reactions were subsequently performed as follows: 42˚C for 60 min; 85˚C for 5 min. The following primers were used for RT: U6, 5'-AAC GCTTCACGAATTTGCGT-3'; miR-183-5p, 5'-CTCAACTGG TGTCGTGGAGTCGGCAATTCAGTTGAGAGTGAATT-3'.

Subsequently, qPCR was performed using GoTaq qPCR Master Mix (Promega Corporation). miRNA expression levels were normalized to the internal reference gene U6 using the U6 snRNA normalization RT-PCR quantitation kit (Shanghai GenePharma Co., Ltd.) and the ABI Prism7700 detection system (Applied Biosystems; Thermo Fisher Scientific, Inc.). The qPCR amplification reactions were subsequently performed as follows: 95˚C for 3 min; and 40 cycles at 95˚C for 10 sec, 58˚C for 30 sec and 72˚C for 30 sec. The following primers were used for qPCR: U6 forward, 5'-GCTTCGGCA GCACATATACTAAAAT-3' and reverse, 5'-CGCTTCACG AATTTGCGTGTCAT-3'; and miR-106a-5p forward, 5'-AAA AGTGCTTACAGTGCAGGTAG-3' and reverse, 5'-GAA AAGTGCTTACAGTGCAGGT-3'. miRNA expression levels were quantified using the $2^{-\Delta\Delta Cq}$ method (35).
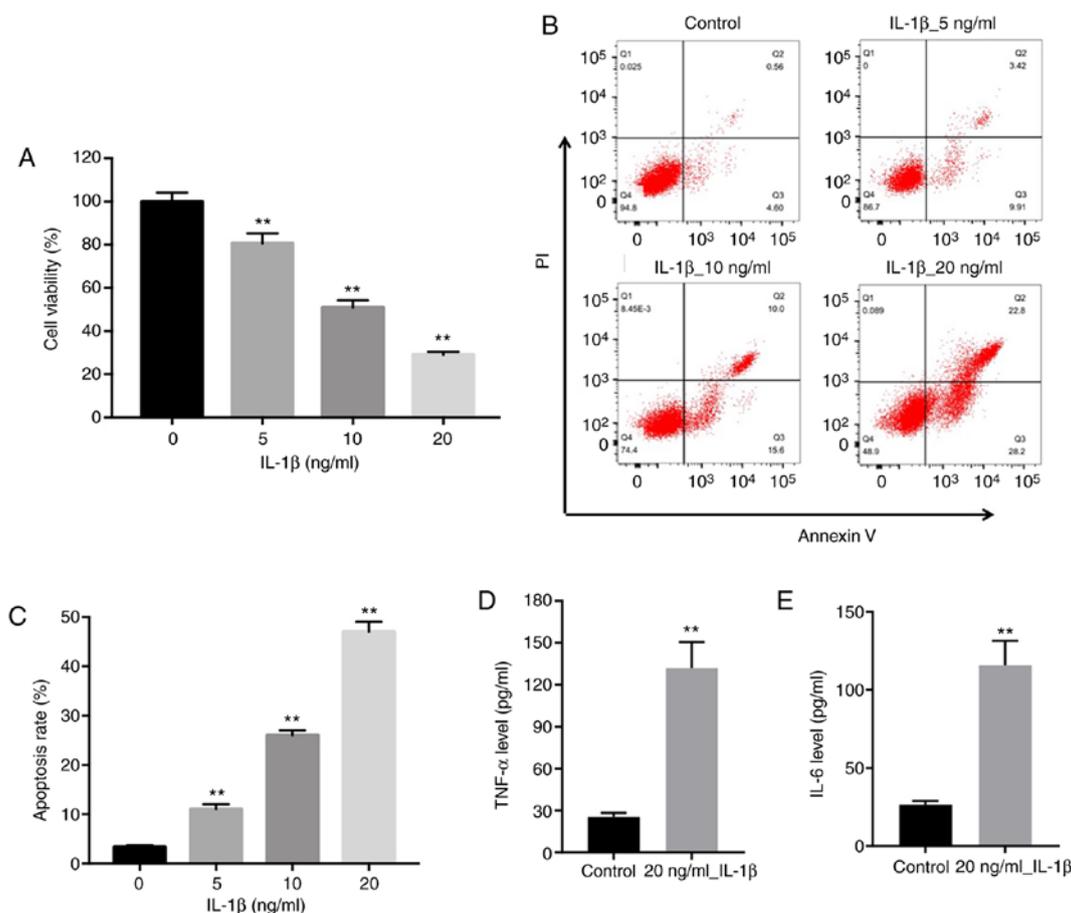
Figure 1. Establishment of an *in vitro* osteoarthritis model. (A) Cell viability was assessed by conducting the Cell Counting Kit-8 assay. CHON-001 cell apoptosis was (B) determined by flow cytometry and (C) quantified. Levels of (D) TNF-α and (E) IL-6 were evaluated by performing ELISAs. **P<0.01 vs. control (0 ng/ml IL-1β). TNF-α, tumor necrosis factor-α; IL, interleukin; PI, propidium iodide.

Western blotting. Following transfection and treatment with BAI and IL-1β, total protein was extracted from CHON-001 cells using RIPA buffer (Beyotime Institute of Biotechnology) for 30 min on ice. Total protein was quantified using a BCA protein kit (Thermo Fisher Scientific, Inc.). Proteins (30 µg) were separated via 10% SDS-PAGE (Pierce; Thermo Fisher Scientific, Inc.), transferred onto PVDF membranes and blocked with 5% non-fat milk (diluted in 0.05% TBS-Tween-20) for 1 h at room temperature. Subsequently, the membranes were incubated at 4˚C overnight with the following primary antibodies: Rabbit anti-Bax (1:1,000; cat. no. ab32503), rabbit anti-caspase-3 (1:1,000; cat. no. ab2302), rabbit anti-Bcl-2 (1:1,000; cat. no. ab32124), rabbit anti-collagen I (1:5,000; cat. no. ab34710), rabbit anti-collagen III (1:1,000; cat. no. ab184993), rabbit anti-aggrecan (1:1,000; cat. no. ab36861), rabbit anti-MMP-13 (1:5,000; cat. no. ab39012), rabbit anti-MMP-9 (1:1,000; cat. no. ab38898), rabbit anti-Notch1 (1:1,000; cat. no. ab52627), rabbit anti-Hes family BHLH transcription factor 1 (Hes1; 1:1,000; cat. no. ab71559) and anti-β-actin (1:1,000; cat. no. ab8227). The membranes were washed with TBS buffer containing 0.05% Tween-20 for 30 min and incubated with a horseradish peroxidase-conjugated goat anti-rabbit secondary antibody (1:5,000; cat. no. ab205718) for 1 h at room temperature. All primary and secondary antibodies were purchased from Abcam. Protein bands were visualized using the Pierce™ ECL Western Blotting Substrate kit (Thermo Fisher Scientific, Inc.) and the Bio-Rad ChemiDoc Imaging system (Bio-Rad Laboratories, Inc.). Protein expression levels were quantified using Image Lab software (version 5.2.1; Bio-Rad Laboratories, Inc.) with β-actin as the loading control.

Statistical analysis. Experiments were repeated ≥3 times. Data are presented as the mean ± standard deviation. Statistical analyses were conducted using GraphPad Prism software (version 7; GraphPad Software, Inc.). Comparisons between two groups were evaluated using unpaired Student's t-test. Comparisons among multiple groups were analyzed by one-way ANOVA followed by Tukey's post hoc test. P<0.05 was considered to indicate a statistically significant difference.

Results

Establishment of an in vitro OA model. To construct an *in vitro* OA model, CHON-001 cells were treated with different concentrations of IL-1β (0, 5, 10 and 20 ng/ml) for 24 h. The CCK-8 assay was conducted to assess the effects of IL-1β on chondrocyte viability. IL-1β inhibited CHON-001 cell viability in a dose-dependent manner compared with the control group (0 ng/ml IL-1β), and 20 ng/ml IL-1β inhibited cell viability by ~70%; therefore, 20 ng/ml IL-1β was selected to establish the *in vitro* OA model in CHON-001 cells (Fig. 1A). The flow
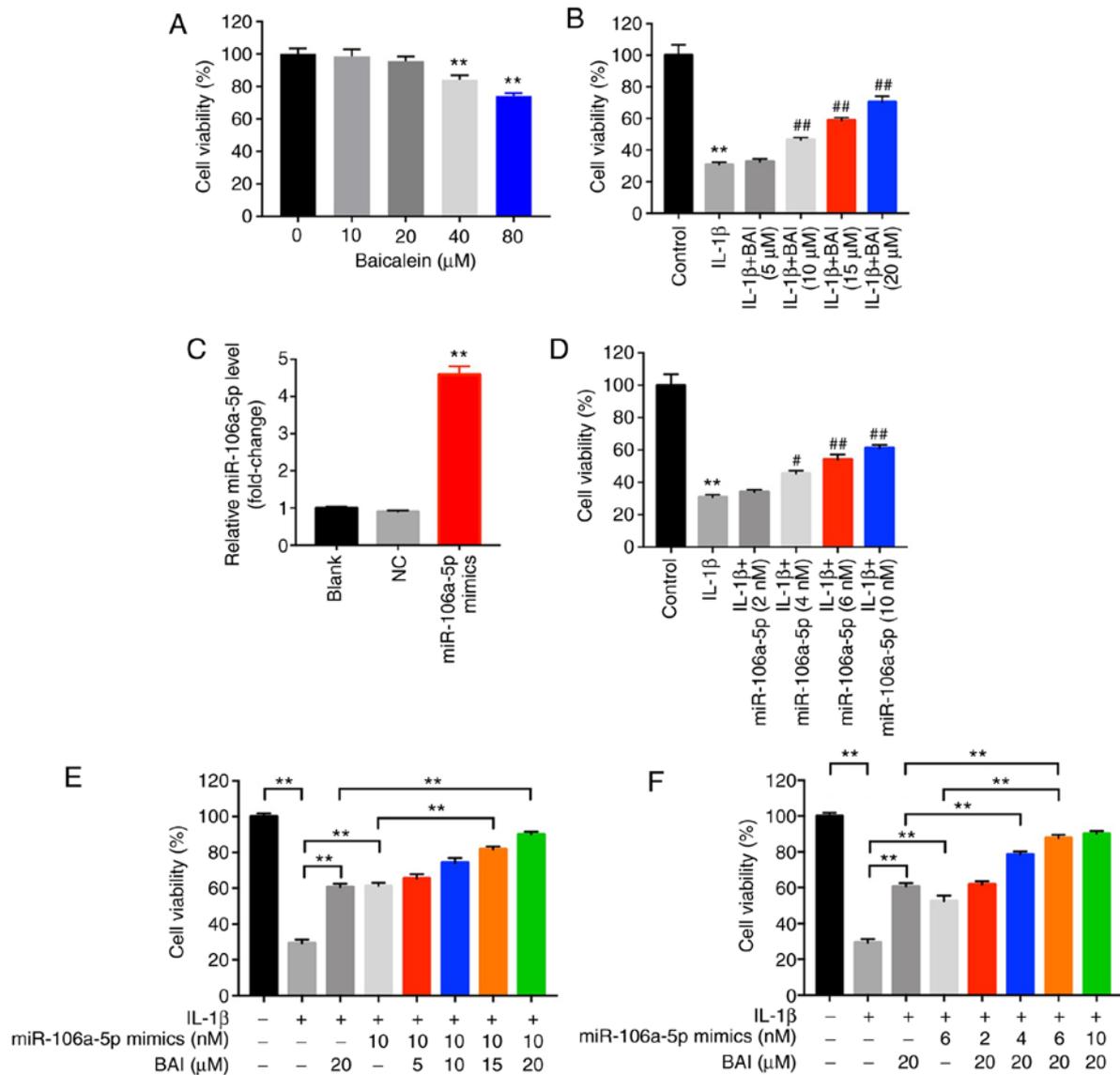
Figure 2. Combination of BAI and miR-106a-5p mimics significantly alleviated IL-1β-induced reductions in cell viability. The effect of (A) BAI and (B) BAI + IL-1β on cell viability. [**]P<0.01 vs. control; [##]P<0.01 vs. IL-1β. (C) Transfection efficiency of miR-106a-5p mimics. [**]P<0.01 vs. NC (D) The effect of IL-1β and miR-106a-5p mimics on cell viability. [**]P<0.01 vs. control; [#]P<0.05 and [##]P<0.01 vs. IL-1β. The effect of different concentrations of (E) BAI and (F) miR-106a-3p mimics on cell viability in IL-1β-treated CHON-001 cells. [**]P<0.01 BAI, baicalein; miR, microRNA; IL, interleukin; NC, negative control.

cytometry results indicated that 5, 10 and 20 ng/ml IL-1β significantly induced CHON-001 cell apoptosis compared with the control group (0 ng/ml IL-1β), with the 20 ng/ml IL-1β group displaying the highest level of apoptosis among the groups (Fig. 1B). As indicators of a functional cellular OA model, the expression levels of inflammatory cytokines, such as TNF-α and IL-6, were significantly increased by 20 ng/ml IL-1β compared with the control group (Fig. 1D and E). Collectively, the results indicated the successful establishment of an *in vitro* OA cell model.

BAI and miR-106a-5p combination treatment significantly alleviates IL-1β-induced inhibition of cell viability. CHON-001 cells were cultured with various concentrations of BAI (0, 10, 20, 40 and 80 µM). The CCK-8 assay results indicated that 40 µM BAI significantly reduced cell viability compared with the control group (0 µg/ml BAI), so 20 µM BAI was used for subsequent experiments (Fig. 1A). The effect of BAI on the OA model

was assessed by measuring cell viability. BAI dose-dependently reversed IL-1β-induced reductions in cell viability. In addition, CHON-001 cells were transfected with miR-106a-5p mimics and the RT-qPCR results indicated transfection efficiency (Fig. 2C). miR-106a-5p mimics also dose-dependently reversed IL-1β-induced reductions in cell viability (Fig. 2D).

Subsequently, the anti-OA effects of BAI and miR-106a-5p mimics were assessed (Fig. 2E and F). The results indicated that 4 nM miR-106a-5p mimics + 20 µM BAI and 6 nM miR-106a-5p mimics + 20 µM BAI displayed an enhanced protective effect in IL-1β-induced CHON-001 cells compared with 20 µM BAI treatment alone. Therefore, the results suggested that combination therapy may synergistically alleviate IL-1β-induced CHON-001 cytotoxicity; however, some combination strategies may only exhibit additive therapeutic effect in OA.

BAI and miR-106a-5p combination treatment significantly alleviates IL-1β-induced apoptosis. An *in vitro* OA
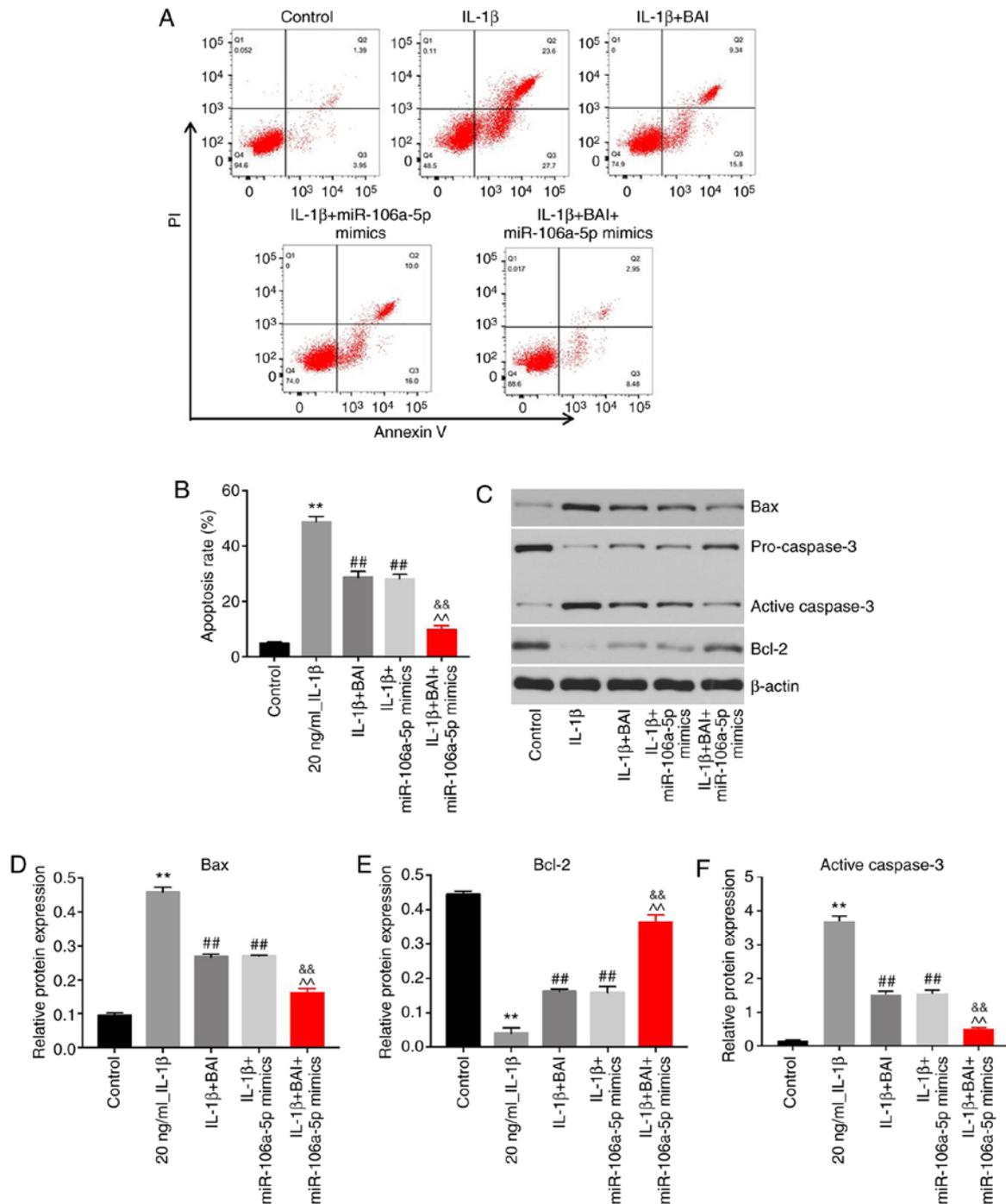
Figure 3. Combination of BAI and miR-106a-5p mimics significantly alleviated IL-1β induced cell apoptosis. Cell apoptosis was (A) determined by flow cytometry and (B) quantified. Protein expression levels were (C) determined by western blotting and semi-quantified for (D) Bax, (E) Bcl-2 and (F) active caspase-3. **P<0.01 vs. control; $^{##}$P<0.01 vs. IL-1β_20 ng/ml; $^{^^}$P<0.01 vs. IL-1β + miR-106a-5p; $^{&&}$P<0.01 vs. IL-1β + BAI. BAI, baicalein; miR, microRNA; IL, interleukin; PI, propidium iodide.

model was established and treated with BAI, miR-106a-5p mimics or a combination. The effects of the combination treatment on apoptosis were assessed via flow cytometry. Monotherapy with BAI or miR-106a-5p mimics significantly alleviated IL-1β-induced CHON-001 cell apoptosis (Fig. 3A and B). Moreover, combination treatment with BAI and miR-106a-5p mimics further reversed IL-1β-induced CHON-001 cell apoptosis compared with either treatment alone. Furthermore, the expression levels of apoptosis-related proteins (Bax and active caspase-3) were

significantly downregulated in the combination treatment group compared with the BAI and miR-106a-5p mimics monotherapy groups (Fig. 3C, D and F). By contrast, the expression level of the anti-apoptotic protein Bcl-2 was significantly upregulated in the combination treatment group compared with the BAI and miR-106a-5p mimics monotherapy groups (Fig. 3E).

BAI and miR-106a-5p combination treatment significantly alleviates the OA phenotype and attenuates the inflammatory
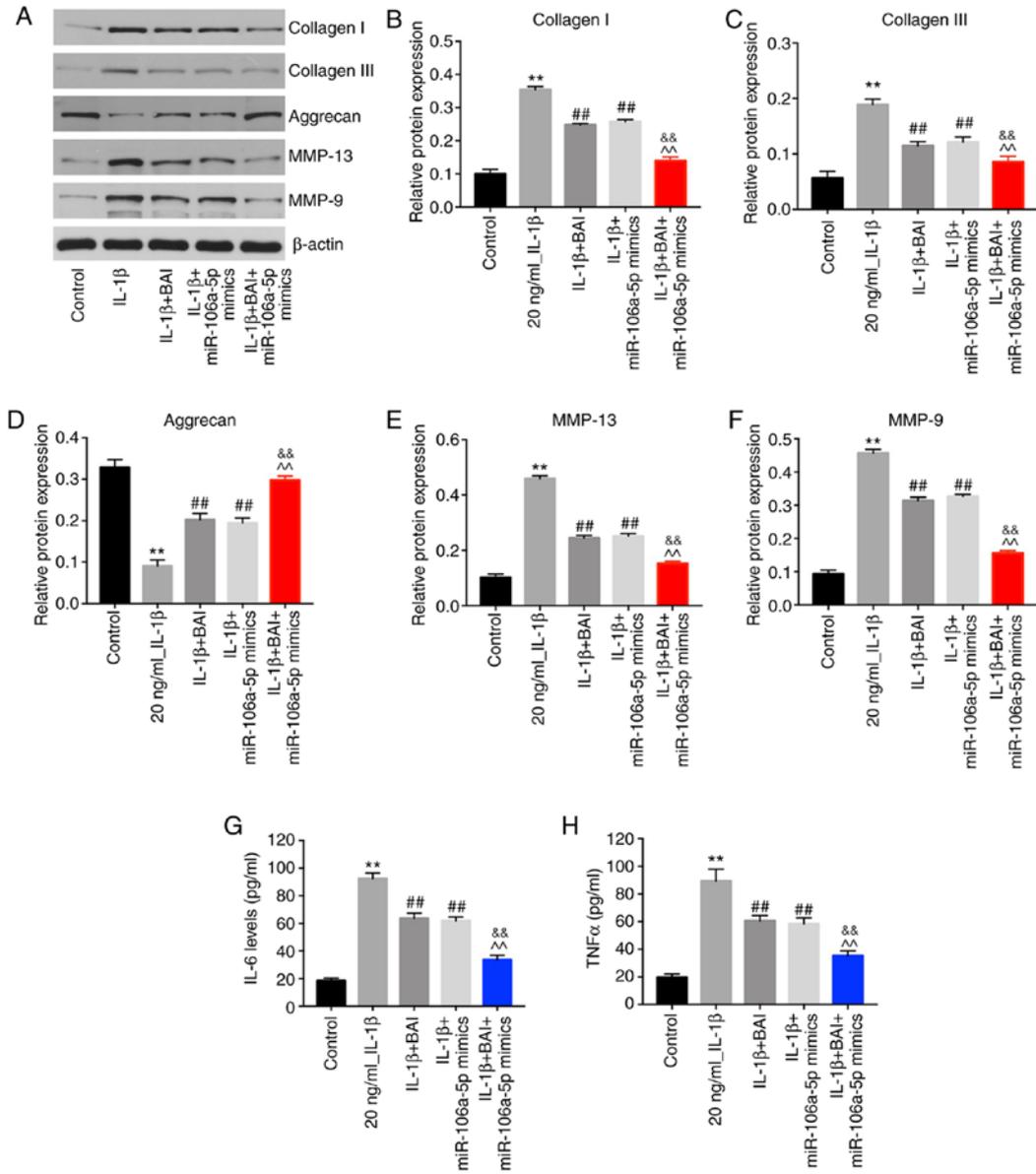
Figure 4. Combination of BAI and miR-106a-5p mimics significantly alleviated the osteoarthritis phenotype and reversed the inflammatory response. Protein expression levels were (A) determined by western blotting and semi-quantified for (B) collagen I, (C) collagen III, (D) aggrecan, (E) MMP-13 and (F) MMP-9. (G) IL-6 and (H) TNF-α levels were evaluated using ELISAs. **P<0.01 vs. control; ##P<0.01 vs. IL-1β_20 ng/ml; ^^P<0.01 vs. IL-1β + miR-106a-5p; &&P<0.01 vs. IL-1β + BAI. BAI, baicalein; miR, microRNA; MMP, matrix metallopeptidase; IL, interleukin; TNF-α, tumor necrosis factor-α.
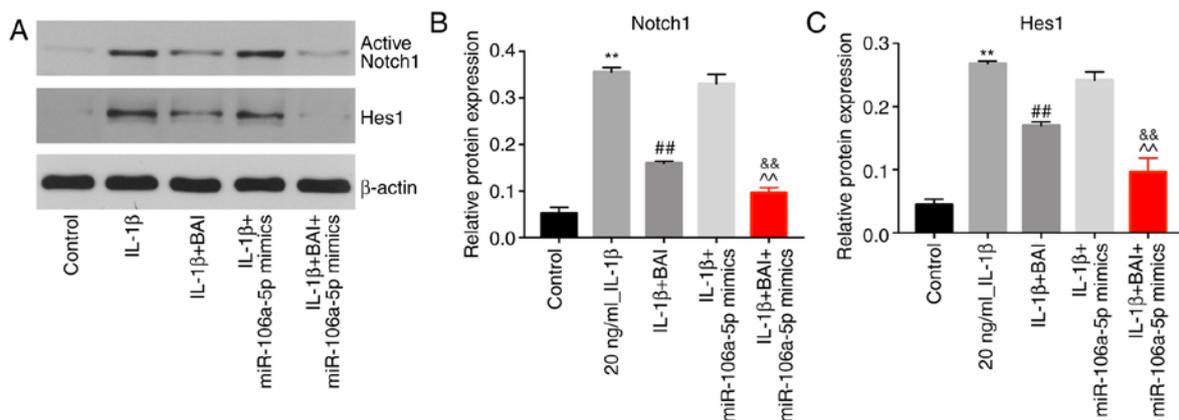
Figure 5. Combination of BAI and miR-106a-5p mimics reversed IL-1β-mediated upregulation of active Notch1 and Hes1. Protein expression levels were (A) determined by western blotting and semi-quantified for (B) active Notch1 and (C) Hes1. **P<0.01 vs. control; ##P<0.01 vs. IL-1β_20 ng/ml; ^^P<0.01 vs. IL-1β + miR-106a-5p; &&P<0.01 vs. IL-1β + BAI. BAI, baicalein; miR, microRNA; IL, interleukin; Hes1, hes family bHLH transcription factor 1.

response. To determine the phenotype of the OA model, the expression levels of collagen I and III, aggrecan, MMP-13 and MMP-9 were detected by western blotting. BAI or miR-106a-5p mimics monotherapy reversed IL-1β-induced aggrecan degradation, but combination therapy was more effective compared with either monotherapy (Fig. 4A and D). Moreover, IL-1β-induced upregulation of collagen I and III was alleviated to a greater extent in the combination treatment group compared with the BAI and miR-106a-5p mimics monotherapy groups (Fig. 4A-C). Similarly, combination treatment reversed IL-1β-mediated upregulation of MMP-9 and MMP-13 to a greater extent compared with the BAI and miR-106a-5p mimics monotherapy groups (Fig. 4A, E and F). In addition, the combination treatment group displayed lower levels of TNF-α and IL-6 compared with the BAI and miR-106a-mimics monotherapy groups (Fig. 4G and H). Collectively, the results indicated that the inflammatory response of the OA model was reversed to a greater degree by combination treatment compared with BAI or miR-106a-5p mimics monotherapy.

BAI and miR-106a-5p combination treatment reverses IL-1β-induced upregulation of active Notch1 and Hes1. IL-1β significantly upregulated active Notch1 expression in CHON-001 cells compared with the control group, but BAI treatment significantly reversed IL-1β-mediated upregulation in the *in vitro* OA model. By contrast, miR-106a-5p mimics did not inhibit IL-1β-induced upregulation of active Notch1. BAI and miR-106a-5p combination treatment alleviated IL-1β-mediated upregulation of active Notch1 to a greater degree compared with BAI treatment alone (Fig. 5A and B). The protein expression level of Hes1 was also upregulated in the IL-1β group compared with the control group (Fig. 5A and C), which was reversed following treatment with BAI, but not miR-106a-5p mimics. However, the combination of BAI and miR-106a-5p mimics had a greater inhibitory effect on IL-1β-mediated Hes1 upregulation compared with BAI alone (Fig. 5A and C).

Discussion

The present study indicated that combination treatment of BAI and miR-106a-5p mimics attenuated the OA phenotype by reversing IL-1β-induced upregulation of active Notch 1 and Hes 1. Consistent with the results of the present study, previous studies have reported that BAI exhibited an antitumor effect via downregulation of the Notch 1/Hes 1 signaling pathway. Lian *et al* (36) indicated that BAI could inhibit cervical cancer cell proliferation via inhibition of the Notch 1/Hes signaling pathway. Similarly, Su *et al* (37) reported that the antitumor effect of BAI was also mediated via downregulation of Notch1 and Hes 1 expression in non-small cell lung carcinoma A549 and H1299 cells. The aforementioned studies and the present study identified a common mechanism underlying BAI-mediated therapeutic effects in multiple diseases. However, Ji *et al* (32) suggested that different signaling pathways and targets are involved in miR-106a-5p-associated OA pathogenesis. According to the aforementioned study, miR-106a-5p downregulation was accompanied by decreased paired box protein PAX-5 expression and increased GLI-similar 3 expression in

patients with OA. The discrepancy between studies may be due to the complexity of the signaling pathways involved in OA pathogenesis.

Interestingly, Pu *et al* (38) demonstrated that BAI inhibited acinar-to-ductal metaplasia of AR42J pancreatic acinal cells via inhibiting NF-κB activation. In the present study, it was revealed that BAI treatment exhibited an effect on Notch signaling in IL-1β-treated CHON-001 cells. The Notch 1/Hes 1 signaling pathway might be a common mechanism underlying several protective effects of BAI against a number of diseases. Different signaling pathways might be involved when BAI is used for the treatment of other diseases. Therefore, the results of the present study provide an insight into investigating the different mechanisms underlying BAI in different diseases. Since the signaling pathways and targets involved in OA pathogenesis are numerous and complex (39,40), further *in vitro* and *in vivo* studies are required to determine the mechanisms underlying the effects of combined treatment with BAI and miR-106a-5p mimics.

In conclusion, the present study suggested that the combined treatment of BAI and miR-106a-5p mimics might achieve an improved anti-inflammatory and antiapoptotic effect in IL-1β-stimulated CHON-001cells.

Acknowledgements

Not applicable.

Funding

Availability of data and materials

The datasets used and/or analyzed during the current study are available from the corresponding author on reasonable request.

Authors' contributions

QX made major contributions to the conception, design and manuscript drafting of the present study. JW and TW were responsible for data acquisition, data analysis and data interpretation. HZ made substantial contributions to conception and design of the study and revised the manuscript. All authors agreed to be accountable for all aspects of the work. All authors read and approved the final manuscript.

Ethics approval and consent to participate

Not applicable.

Patient consent for publication

Not applicable.

Competing interests

The authors declare that they have no competing interests.

References

1. Rustenburg CME, Emanuel KS, Peeters M, Lems WF, Vergroesen PA and Smit TH: Osteoarthritis and intervertebral disc degeneration: Quite different, quite similar. JOR Spine 1: e1033, 2018.
2. Gezginaslan O, Ozturk EA, Cengiz M, Mirzaoglu T and Cakci FA: Effects of isokinetic muscle strengthening on balance, proprioception, and physical function in bilateral knee osteoarthritis patients with moderate fall risk. Turk J Phys Med Rehabil 64: 353-361, 2018.
3. Berenbaum F: Osteoarthritis as an inflammatory disease (osteoarthritis is not osteoarthrosis!). Osteoarthritis Cartilage 21: 16-21, 2013.
4. Blagojevic M, Jinks C, Jeffery A and Jordan KP: Risk factors for onset of osteoarthritis of the knee in older adults: A systematic review and meta-analysis. Osteoarthritis Cartilage 18: 24-33, 2010.
5. Fang Y, Wang P, Xia L, Bai S, Shen Y, Li Q, Wang Y, Zhu J, Du J and Shen B: Aberrantly hydroxymethylated differentially expressed genes and the associated protein pathways in osteoarthritis. PeerJ 7: e6425, 2019.
6. Duval E, Leclercq S, Elissalde JM, Demoor M, Galera P and Boumediene K: Hypoxia-inducible factor 1alpha inhibits the fibroblast-like markers type I and type III collagen during hypoxia-induced chondrocyte redifferentiation: Hypoxia not only induces type II collagen and aggrecan, but it also inhibits type I and type III collagen In the hypoxia-inducible factor 1alpha-dependent redifferentiation of chondrocytes. Arthritis Rheum 60: 3038-3048, 2009.
7. Egloff C, Hart DA, Hewitt C, Vavken P, Valderrabano V and Herzog W: Joint instability leads to long-term alterations to knee synovium and osteoarthritis in a rabbit model. Osteoarthritis Cartilage 24: 1054-1060, 2016.
8. Chen WP, Xiong Y, Hu PF, Bao JP and Wu LD: Baicalein inhibits MMPs expression via a MAPK-dependent mechanism in chondrocytes. Cell Physiol Biochem 36: 325-333, 2015.
9. Ruan G, Xu J, Wang K, Wu J, Zhu Q, Ren J, Bian F, Chang B, Bai X, Han W and Ding C: Associations between knee structural measures, circulating inflammatory factors and MMP13 in patients with knee osteoarthritis. Osteoarthritis Cartilage 26: 1063-1069, 2018.
10. Fei J, Liang B, Jiang C, Ni H and Wang L: Luteolin inhibits IL-1β-induced inflammation in rat chondrocytes and attenuates osteoarthritis progression in a rat model. Biomed Pharmacother 109: 1586-1592, 2019.
11. Marchand F, Perretti M and McMahon SB: Role of the immune system in chronic pain. Nat Rev Neurosci 6: 521-532, 2005.
12. Stassen M, Hultner L and Schmitt E: Classical and alternative pathways of mast cell activation. Crit Rev Immunol 22: 115-140, 2002.
13. Shen J, Abu-Amer Y, O'Keefe RJ and McAlinden A: Inflammation and epigenetic regulation in osteoarthritis. Connect Tissue Res 58: 49-63, 2017.
14. Kim L and Kim JY: Chondroprotective effect of curcumin and lecithin complex in human chondrocytes stimulated by IL-1β via an anti-inflammatory mechanism. Food Sci Biotechnol 28: 547-553, 2019.
15. Hosaka Y, Saito T, Sugita S, Hikata T, Kobayashi H, Fukai A, Taniguchi Y, Hirata M, Akiyama H, Chung UI and Kawaguchi H: Notch signaling in chondrocytes modulates endochondral ossification and osteoarthritis development. Proc Natl Acad Sci USA 110: 1875-1880, 2013.
16. Gao W, Sweeney C, Walsh C, Rooney P, McCormick J, Veale DJ and Fearon U: Notch signalling pathways mediate synovial angiogenesis in response to vascular endothelial growth factor and angiopoietin 2. Ann Rheum Dis 72: 1080-1088, 2013.
17. Mirando AJ, Liu Z, Moore T, Lang A, Kohn A, Osinski AM, O'Keefe RJ, Mooney RA, Zuscik MJ and Hilton MJ: RBP-Jκ-dependent Notch signaling is required for murine articular cartilage and joint maintenance. Arthritis Rheum 65: 2623-2633, 2013.
18. Wang W, Zeng L, Wang ZM, Zhang S, Rong XF and Li RH: Ginsenoside Rb1 inhibits matrix metalloproteinase 13 through down-regulating Notch signaling pathway in osteoarthritis. Exp Biol Med (Maywood) 240: 1614-1621, 2015.
19. Yu HT, Gu CZ and Chen JQ: MiR-9 facilitates cartilage regeneration of osteoarthritis in rabbits through regulating Notch signaling pathway. Eur Rev Med Pharmacol Sci 23: 5051-5058, 2019.
20. Li Y, Wang J, Song X, Bai H, Ma T, Zhang Z, Li X, Jiang R, Wang G, Fan X, *et al*: Effects of baicalein on IL-1β-induced inflammation and apoptosis in rat articular chondrocytes. Oncotarget 8: 90781-90795, 2017.
21. Chi YS, Lim H, Park H and Kim HP: Effects of wogonin, a plant flavone from Scutellaria radix, on skin inflammation: In vivo regulation of inflammation-associated gene expression. Biochem Pharmacol 66: 1271-1278, 2003.
22. Gao Z, Huang K, Yang X and Xu H: Free radical scavenging and antioxidant activities of flavonoids extracted from the radix of *Scutellaria baicalensis Georgi*. Biochim Biophys Acta 1472: 643-650, 1999.
23. Huang Y, Tsang SY, Yao X and Chen ZY: Biological properties of baicalein in cardiovascular system. Curr Drug Targets Cardiovasc Haematol Disord 5: 177-184, 2005.
24. Wang CZ, Mehendale SR and Yuan CS: Commonly used antioxidant botanicals: Active constituents and their potential role in cardiovascular illness. Am J Chin Med 35: 543-558, 2007.
25. Zhang X, Zhu Y, Chen X, Zhang Y, Zhang Y, Jia Y, Wang H, Liu Y and Xiao L: Baicalein ameliorates inflammatory-related apoptotic and catabolic phenotypes in human chondrocytes. Int Immunopharmacol 21: 301-308, 2014.
26. Hamam R, Hamam D, Alsaleh KA, Kassem M, Zaher W, Alfayez M, Aldahmash A and Alajez NM: Circulating microRNAs in breast cancer: Novel diagnostic and prognostic biomarkers. Cell Death Dis 8: e3045, 2017.
27. Skommer J, Rana I, Marques FZ, Zhu W, Du Z and Charchar FJ: Small molecules, big effects: The role of microRNAs in regulation of cardiomyocyte death. Cell Death Dis 5: e1325, 2014.
28. McDermott R, Gabikian P, Sarvaiya P, Ulasov I and Lesniak MS: MicroRNAs in brain metastases: Big things come in small packages. J Mol Med (Berl) 91: 5-13, 2013.
29. Bak RO, Hollensen AK and Mikkelsen JG: Managing microRNAs with vector-encoded decoy-type inhibitors. Mol Ther 21: 1478-1485, 2013.
30. Xu JF, Zhang SJ, Zhao C, Qiu BS, Gu HF, Hong JF, Cao L, Chen Y, Xia B, Bi Q and Wang YP: Altered microRNA expression profile in synovial fluid from patients with knee osteoarthritis with treatment of hyaluronic acid. Mol Diagn Ther 19: 299-308, 2015.
31. Le LT, Swingler TE, Crowe N, Vincent TL, Barter MJ, Donell ST, Delany AM, Dalmay T, Young DA and Clark IM: The microRNA-29 family in cartilage homeostasis and osteoarthritis. J Mol Med (Berl) 94: 583-596, 2016.
32. Ji Q, Qi D, Xu X, Xu Y, Goodman SB, Kang L, Song Q, Fan Z, Maloney WJ and Wang Y: Cryptotanshinone protects cartilage against developing osteoarthritis through the miR-106a-5p/GLIS3 axis. Mol Ther Nucleic Acids 11: 170-179, 2018.
33. Guan YJ, Li J, Yang X, Du S, Ding J, Gao Y, Zhang Y, Yang K and Chen Q: Evidence that miR-146a attenuates aging- and trauma-induced osteoarthritis by inhibiting Notch1, IL-6, and IL-1 mediated catabolism. Aging Cell 17: e12752, 2018.
34. Hu G, Zhao X, Wang C, Geng Y, Zhao J, Xu J, Zuo B, Zhao C, Wang C and Zhang X: MicroRNA-145 attenuates TNF-α-driven cartilage matrix degradation in osteoarthritis via direct suppression of MKK4. Cell Death Dis 8: e3140, 2017.
35. Livak KJ and Schmittgen TD: Analysis of relative gene expression data using real-time quantitative PCR and the 2(-Delta Delta C(T)) method. Methods 25: 402-408, 2001.
36. Lian H, Hui Y, Xiaoping T, Wei T, Jiyi X and Xiaolan Y: Baicalein suppresses the proliferation of human cervical cancer cells via Notch 1/Hes signaling pathway. J Cancer Res Ther 15: 1216-1220, 2019.
37. Su G, Chen H and Sun X: Baicalein suppresses non small cell lung cancer cell proliferation, invasion and Notch signaling pathway. Cancer Biomark 22: 13-18, 2018.
38. Pu WL, Luo YY, Bai RY, Guo AW, Zhou K, Zhang YS, Miao L, Rüegg C, Hottiger MO, Gao XM and Sun LK: Baicalein inhibits acinar-to-ductal metaplasia of pancreatic acinal cell AR42J via improving the inflammatory microenvironment. J Cell Physiol 233: 5747-5755, 2018.
39. Saito T and Tanaka S: Molecular mechanisms underlying osteoarthritis development: Notch and NF-κB. Arthritis Res Ther 19: 94, 2017.
40. Zhou Y, Wang T, Hamilton JL and Chen D: Wnt/β-catenin signaling in osteoarthritis and in other forms of arthritis. Curr Rheumatol Rep 19: 53, 2017.